Fetal brain hypometabolism during prolonged hypoxaemia in the llama

Germán Ebensperger[1], Renato Ebensperger[1], Emilio A. Herrera[1], Raquel A. Riquelme[2], Emilia M. Sanhueza[1], Florian Lesage[3], Juan J. Marengo[1], Rodrigo I. Tejo[1], Aníbal J. Llanos[1,4] and Roberto V. Reyes[1]

[1] *Programa de Fisiopatología, Instituto de Ciencias Biomédicas (ICBM), Facultad de Medicina, Universidad de Chile, Santiago, Chile*
[2] *Departamento de Bioquímica y Biología Molecular, Facultad de Ciencias Químicas y Farmacéuticas, Universidad de Chile, Santiago, Chile*
[3] *Institut de Pharmacologie Moléculaire et Cellulaire, CNRS, Sophia-Antipolis, Valbonne, France*
[4] *Centro Internacional de Estudios Andinos (INCAS), Universidad de Chile, Santiago, Chile*

In this study we looked for additional evidence to support the hypothesis that fetal llama reacts to hypoxaemia with adaptive brain hypometabolism. We determined fetal llama brain temperature, Na^+ and K^+ channel density and Na^+–K^+-ATPase activity. Additionally, we looked to see whether there were signs of cell death in the brain cortex of llama fetuses submitted to prolonged hypoxaemia. Ten fetal llamas were instrumented under general anaesthesia to measure pH, arterial blood gases, mean arterial pressure, heart rate, and brain and core temperatures. Measurements were made 1 h before and every hour during 24 h of hypoxaemia ($n = 5$), which was imposed by reducing maternal inspired oxygen fraction to reach a fetal arterial partial pressure of oxygen (P_{a,O_2}) of about 12 mmHg. A normoxaemic group was the control ($n = 5$). After 24 h of hypoxaemia, we determined brain cortex Na^+–K^+-ATPase activity, ouabain binding, and the expression of NaV1.1, NaV1.2, NaV1.3, NaV1.6, TREK1, TRAAK and K_{ATP} channels. The lack of brain cortex damage was assessed as poly ADP-ribose polymerase (PARP) proteolysis. We found a mean decrease of 0.56°C in brain cortex temperature during prolonged hypoxaemia, which was accompanied by a 51% decrease in brain cortex Na^+–K^+-ATPase activity, and by a 44% decrease in protein content of NaV1.1, a voltage-gated Na^+ channel. These changes occurred in absence of changes in PARP protein degradation, suggesting that the cell death of the brain was not enhanced in the fetal llama during hypoxaemia. Taken together, these results provide further evidence to support the hypothesis that the fetal llama responds to prolonged hypoxaemia with adaptive brain hypometabolism, partly mediated by decreases in Na^+–K^+-ATPase activity and expression of NaV channels.

Corresponding author R. V. Reyes: Programa de Fisiopatología, Instituto de Ciencias Biomédicas, Facultad de Medicina, Universidad de Chile, Casilla 16038, Santiago 9, Chile. Email: vicreyes@med.uchile.cl

A few mammalian species, such as diving mammals and the mammals that live in the low-oxygen environment of high altitudes, e.g. the South American *Camelidae*, can thrive during prolonged periods of oxygen shortage. To live at high altitudes, *Camelidae* have evolved strategies that are apparently genetically determined, since they are maintained in animals born and living at sea level. In llamas, a domestic *Camelidae*, these adaptations include low haemoglobin P_{50} (partial pressure of oxygen where half of the oxygen binding sites are saturated with oxygen), small elliptical red cells with high haemoglobin concentration, a slight increase in blood haemoglobin concentration, high muscle myoglobin concentration, more efficient oxygen extraction, and high lactic dehydrogenase activity, compared with low-altitude species (Llanos *et al.* 2003). In addition, the llama maintains a low pulmonary arterial pressure, with an absence of highly muscularized pulmonary arterioles, despite living at very high altitudes (Harris *et al.* 1982).

Fetal life imposes an additional oxygen challenge to high altitude mammals. Fetal arterial partial pressure of oxygen (P_{a,O_2}) is 30 mmHg in the umbilical vein at sea level, and is much lower in high-altitude pregnancies. Compared with fetuses of lowland species, such as sheep, the fetal llama also has low haemoglobin P_{50} (Moraga *et al.* 1996), lower basal cardiac output and organ blood flow (Llanos *et al.* 2003),

G. Ebensperger and R. Ebensperger contributed equally to this work.

and a more efficient total oxygen extraction (Benavides *et al.* 1989). Remarkably, unlike fetuses of lowland species, the llama fetus responds to acute hypoxaemia with only a minor increase in cerebral blood flow (Llanos *et al.* 2003). Furthermore, the fetal llama shows a progressive fall in brain oxygen delivery and cerebral oxygen consumption with progression of the fetal hypoxaemia (Llanos *et al.* 2002). We have shown that the electrocorticogram flattens under these conditions of hypoxaemia, and seizure activity does not occur, which suggests that no hypoxaemic damage occurs (Llanos *et al.* 2003).

A pressing question is how the oxygen delivery and consumption can decrease in the fetal llama brain during hypoxaemia, without concomitant damage. One possible explanation is that the neurones undergo hypometabolism during the hypoxaemic episode. In the neurone, more than 50% of energy expenditure is due to the continuous ion pumping needed to maintain the ion electrochemical gradients, which in turn are needed to support the repetitive opening of Na^+ and K^+ channels, which account for much of the brain's electrical activity (Erecinska & Silver, 1994). In the brain of most vertebrates, ATP rapidly decreases during severe oxygen deprivation; ionic gradients collapse leading to depolarization, followed by a strong and massive intracellular Ca^{2+} increase, and the onset of the cell death events. Nevertheless, some vertebrates, such as an anoxia-tolerant species of turtles (*Trachemys scripta*), have developed adaptive brain hypometabolism as a defence response against anoxia. One of the principal features accounting for brain hypometabolism is the reduction in activity of the Na^+–K^+-ATPase *pari passu*, with a decreased permeability of Na^+ and K^+ ions and/or a lesser expression of Na^+ and K^+ channels in the central nervous system (Hylland *et al.* 1997; Pék-Scott & Lutz, 1998; Bickler & Buck, 1998; Nilsson & Lutz, 2004). An analogous strategy, imposed by the sustained hypobaric hypoxia of life at extreme altitude, may have evolved in the fetal llama to avoid cerebral damage.

In this study, we looked for additional evidence to support the hypothesis that the fetal llama reacts to hypoxaemia with adaptive brain hypometabolism. To further support this contention, we determined whether fetal llama brain temperature decreases, and whether this was associated with a reduction of ion channel density and Na^+–K^+-ATPase activity, with no signs of cell death in the brain cortex of llama fetuses submitted to prolonged hypoxaemia.

Methods

Animals

Ten time-dated pregnant llamas were obtained from the University of Chile farm at the Rinconada de Maipú, which is at 540 m above sea level. Once they had arrived at Santiago (585 m above sea level), the llamas were housed in an open yard with access to food and water *ad libitum*. They were familiarized with the study metabolic cage and laboratory conditions for 1–2 weeks prior to the maternal and fetal instrumentation.

Surgery and instrumentation

Maternal and fetal surgeries were carried out on consecutive days using well-established techniques, which have previously been described in detail (Benavides *et al.* 1989; Llanos *et al.* 1995). Following food and water deprivation for 24 h, the maternal llamas were premedicated with atropine (0.04 mg kg^{-1}, I.M., Atropina Sulphato; Laboratorio Chile, Santiago, Chile). Polyvinyl catheters (1.3 mm i.d.) were placed in the maternal descending aorta and inferior vena cava, via a hindlimb artery and vein, under light general anaesthesia (ketamine, 5 mg kg^{-1} I.M., Ketostop; Drug Pharma-Invetec; and xylazine, 0.4 mg kg^{-1} I.M.; Rompun, Bayer, Santiago, Chile) with additional local infiltration of lidocaine (lignocaine) (2% lidocaine hydrochloride, Dimecaina; Laboratorio Beta, Santiago, Chile). The catheters were then tunnelled subcutaneously to exit at the maternal flank. The following day, the fetuses were surgically prepared under maternal general anaesthesia (5–7 mg kg^{-1} sodium thiopentone (Tiopental Sódico; Laboratorio Biosano SA, Santiago, Chile) for induction, and 0.5–2% halothane in 50:50 O_2 and N_2O for maintenance). Following a midline laparotomy, a fetal hindlimb was withdrawn through a small laparotomy. Polyvinyl catheters (0.8 mm i.d.) were inserted into the fetal aorta via a hindlimb artery and into the inferior vena cava via a hindlimb vein (Giussani *et al.* 1996). The fetal head was exposed through a second hysterotomy to position thermistors (Puig Ingeniería y Tecnologías, Santiago, Chile; resolution of 0.02°C, in the range between 35 and 40°C) to measure brain and core temperatures. The thermistor for recording the cerebral temperature was implanted through a small hole drilled in the skull, 1.5 cm anterior to the lambdoidal suture, and 3 cm lateral to the sagittal suture, overlying the parietal cortex. The thermistor to measure core temperature was placed in the right atrium entering through the jugular vein. A catheter was placed in the amniotic cavity for pressure reference, and the uterine and abdominal incisions were closed. All catheters were filled with heparinized saline (1000 IU ml^{-1} heparin in 0.9% NaCl) and plugged with a copper wire. Catheters and cable wires were exteriorized through the incision in the maternal flank, and kept in a pouch sewn onto the maternal skin. During surgery, all llamas were constantly hydrated with a warm intravenous solution of 0.9% NaCl at a rate of 15–20 ml kg^{-1} h^{-1} to compensate for fluid loss during the procedures. At the end of

the surgery, cephazolin (500 mg, Cefazolina; Laboratorio Bestpharma SA, Santiago, Chile) and gentamicin (80 mg, Gentamicina Sulphato, Laboratorio Biosano SA) were given intra-amniotically. After surgery, the animals received cephazolin 1 g and sodium metamizol 20 mg kg^{-1} (Dipirona; Laboratorio Sanderson SA, Santiago, Chile) I.V., each for 12 h on each of 3 days.

At least 4 days of postoperative recovery were allowed before the experiments were commenced. Patency of vascular catheters was maintained by daily flushing with a heparinized solution of 0.9% NaCl (500 IU ml^{-1} 0.9% NaCl).

All experimental protocols were reviewed and approved by the Faculty of Medicine Ethics Committee of the University of Chile. All animal care, maintenance, procedures and experimentation were performed in accordance with the UK Animals (Scientific Procedures) Act, 1986, and the American Physiological Society 'Guiding Principles for Research Involving Animals and Human Beings' (American Physiological Society, 2002).

Experimental protocol

All experiments were based on a 25 h protocol divided into two periods: 1 h of normoxaemia and 24 h of hypoxaemia. The normoxaemic group ($n = 5$) was monitored for 25 h whilst the pregnant llama breathed air. For the hypoxaemic group ($n = 5$), following 1 h of breathing air (basal), a transparent polyethylene bag loosely tied was placed over the llama's head into which controlled mixture of air, N_2 and CO_2 were passed at $\sim$50 l min^{-1}. Hypoxaemia (9% O_2 and 2–3% CO_2 in N_2) was induced for 24 h in the pregnant llama, which reduced maternal P_{a,O_2} from 92.5 $\pm$ 1.5 mmHg to 66.4 $\pm$ 7.8 mmHg, and haemoglobin saturation from 95.0 $\pm$ 0.4% to 91.3 $\pm$ 1.7%. This, in turn, reduced fetal descending aortic P_{a,O_2} and haemoglobin saturation to about 12 mmHg and 24%, respectively, without altering fetal arterial partial pressure of CO_2 (P_{a,CO_2}). The studies were initiated between 09.00 and 11.00 h, and the room lights were on during the whole study. Heparinized arterial blood samples (0.5 ml) were taken from the mother and fetus at intervals of 60 min during the experimental procedure.

On completion of the experiments, the pregnant llama was submitted to a quick caesarean section under general inhalation anaesthesia (0.5–2% halothane in 50:50 O_2 and N_2O for maintenance). Prior to its extraction, the fetus was anaesthetized and killed with intravenous thiopentone sodium (1 g Tiopental Sódico; Laboratorio Biosano SA) and saturated potassium chloride. Thereafter, the fetus was delivered and weighed, and the fetal brain was immediately extracted and weighed. The brain cortex was dissected, frozen with liquid nitrogen and kept at -80°C until biochemical and molecular biological measurements were performed. Brain cortex samples were frozen during an interval that was no longer than 15 min from completion of the experimental protocol. The parietal cortex around the thermistor did not show macroscopic signs of damage (swelling, haematoma or infarct). The tip of the thermistor inserted through the jugular vein was in the right atrium. No macroscopic damage was observed in the heart.

The maternal llamas were kept alive, and after completion of postoperative care, they were returned to the flock.

Measurement of maternal and fetal cardiorespiratory variables

We measured arterial pH, P_{a,O_2}, P_{a,CO_2} (ABL 555 blood gas monitor; Radiometer, Copenhagen, Denmark; measurements were corrected to 39°C), percentage saturation of haemoglobin, and haemoglobin concentration (OSM3 Hemoximeter; Radiometer).

Blood oxygen content was calculated as follows:

$$O_2 \text{ content (ml } O_2 \text{ dl}^{-1}) = \text{Hb concentration (g dl}^{-1}) \times \text{Hb saturation}/100 \times 1.34 \text{ (ml } O_2 \text{ g}^{-1} \text{ Hb)}.$$

Fetal and maternal arterial and amniotic pressures were recorded continuously throughout the experiment using a data acquisition system connected to a PC (Powerlab/8SP System and Chart v4.1.2 Software; ADInstruments Pty Ltd, New South Wales, Australia). Fetal and maternal heart rate and mean arterial pressure were calculated from these records. Fetal brain and fetal core temperature were measured continuously during the study and recorded in a data acquisition system (Puig Ingeniería y Tecnologías, Santiago, Chile) connected to a PC. Fetal brain temperature minus core temperature was calculated every minute, and the average measurement over 24 h was calculated. The continuously measured and calculated variables were averaged every 60 min of recording, and the hourly values were used to calculate means.

Total brain cortex protein and membrane preparation

For total protein preparation, brain cortex was homogenized in a solution containing (mM) 137 NaCl, 2.7 KCl, 5 EDTA, 8 Na_2HPO_4, 1.5 KH_2PO_4, supplemented with a protease inhibitor cocktail. This was centrifuged at 10 000 *g* for 10 min and the supernatant was recovered. The protein concentration was measured, and the extract was kept in aliquots at -80°C. For membrane preparation, brain cortex was homogenized in 0.32 M sucrose, 10 mM Tris-HCl pH 7.4 supplemented with a protease inhibitor cocktail, and centrifuged at 2000 *g* for 10 min. The supernatant was ultracentrifuged at 100 000 *g* for 60 min to obtain a total-membrane pellet that was resuspended in 50 mM Tris-HCl pH 7.4. The protein concentration was

then measured, and the membrane fraction was kept in aliquots at −80°C.

Brain Na^+–K^+-ATPase activity

The enzymatic activity was measured as the conversion of paranitrophenylphosphate (pNPP) to paranitrophenol (pNP) (Hylland *et al.* 1997). The rate of total pNP formation was measured by incubating 25 μg of membrane protein with 0.25 ml reaction mixture containing (mM) 25 KCl, 10 pNPP, 5 $MgCl_2$, 50 Tris-HCl pH 7.4, and the rate of pNP formation resistant to ouabain inhibition was measured by replacing KCl with 1 mM ouabain. The reactions were carried out at 37°C for 3 min, a period during which both total and ouabain-resistant pNP formation increased linearly. The reaction was stopped by adding 1.5 ml of 0.1 M NaOH, and pNP concentration was measured by spectrophotometry at 410 nm. Na^+–K^+-ATPase activity was calculated as the difference between total and ouabain-resistant pNP formation and expressed as μmol pNP (mg protein)$^{-1}$ min^{-1}.

Ouabain binding

Membrane protein (25 μg) was incubated with [^{3}H]ouabain (0.1–500 nM, 18.0 Ci mmol^{-1}; Perkin Elmer Life Sciences, Boston, USA) in a reaction mixture composed of (mM) 150 NaCl, 5 $MgCl_2$, 1 EDTA-Tris, 1.2 ATP, and 50 Tris-HCl, pH 7.4, at 37°C for 90 min. The reaction was stopped by rapid filtration in Whatman GF/C glass fibre filters, followed by three washings with cold 50 mM Tris-HCl buffer, and the retained radioactivity was counted by liquid scintillation. Non-specific binding was determined by incubation in the presence of 10 μM cold ouabain under identical conditions. The specific binding was calculated as the difference between total and non-specific binding, expressed as pmol (mg protein)$^{-1}$; maximal binding (B_{MAX}) and the dissociation constant (K_D) for ouabain were calculated by fitting specific binding (B) to the function of the form:

$$B = B_{MAX} \times L/K_D + L$$

where L (nM) is the ouabain concentration (Origin 5.0 Software; OriginLab Corporation, Northampton, USA).

Glybenclamide binding

Membrane protein (100 μg) was incubated with [^{3}H]glybenclamide (0.05–16 nM, 50.0 Ci mmol^{-1}; Perkin Elmer Life Sciences) in 50 mM Tris-HCl pH 7.4 at 25°C for 60 min. Non-specific binding was measured by incubating in the presence of 1 μM cold glybenclamide. Filtration, washing, radioactivity measurements and calculations were done as described for ouabain binding.

Immunoblot determinations

Protein (10–50 μg) was resolved by electrophoresis in SDS-polyacrylamide gels and transferred to nitrocellulose membranes under standard conditions (Towbin & Gordon, 1984). The blots were blocked with 4% nonfat milk in phosphate-buffered saline (PBS), and then incubated with one of the following primary antibodies: polyclonal anti-NaV1.1, anti-NaV1.2, anti-NaV1.3, anti-NaV1.6 (all from Alomone Laboratories, Jerusalem, Israel; used at 1:200 dilution), monoclonal antiβ-actin (Clone AC-74; Sigma, St Louis, MO, USA; used at a dilution of 1:5000), or monoclonal anti-PARP (Clone C2-10; BD PharMingen, San Diego, CA, USA; used at a dilution of 1:2000), followed by incubation with HRP-conjugated anti-rabbit IgG or anti-mouse IgG secondary antibodies (both from Jackson Immuno-Research Laboratories, Inc., PA, USA; used at 1:5000 dilution) with washes with PBS/0.1% Tween 20 between primary and secondary antibody incubation. Signals were detected by enhanced chemiluminescence (SuperSignal West Pico Chemiluminescent Substrate; Pierce, Rockford, USA) and autoradiography.

RT-PCR determination

Total RNA was prepared using the SV Total RNA Isolation kit (Promega, Madison, WI, USA) and cDNA was synthesized by reverse transcription using random hexamers and the SuperScript First Strand Synthesis System for RT-PCR kit (Invitrogen Life Technologies, CA, USA). Procedures were carried out following the manufacturers' instructions. PCR amplification of partial sequences of DNA coding for different ion channel subunits was carried out from cDNA synthesized from 0.2 μg of total RNA, with 1 U of *Taq* polymerase (Promega), 10 mM Tris-HCl pH 9.0, 50 mM KCl, 0.1% Triton X-100, 1.5 mM $MgCl_2$, 0.2 mM dNTP mix, and 0.3 μM of each one of the primers under the conditions indicated in Table 1. The PCR products were separated by electrophoresis on ethidium bromide agarose gels, and visualized under UV light.

The bands obtained on immunoblot or RT-PCR determinations were quantified by densitometric analysis using the Scion Image Software (Scion Image Beta 4.02 Win; Scion Corporation, MD, USA).

Statistical analysis

All values are expressed as means ± S.E.M. Changes in the variables measured as a function of time were tested for statistical significance using two-way and one-way ANOVA for repeated measures, followed by the Newman-Keuls test. Comparisons among the groups were

Table 1. Sequences of primers and conditions used for semiquantitative RT-PCR

Target mRNA		Sequence (5′→3′)	Annealing temperature	Amplification cycles	GenBank accession no.	Product size (bp)
NaV 1.1	(S)	gcattgcagaagaaaaagctaagaa	49°C	30	NM_030875	403
	(A)	cctgtgaaggtgtactctacatt			(Rat)	
NaV 1.2	(S)	gatgacgataacgaaatgaacaac	44°C	32	X03639	570
	(A)	tatctgacaacacttgaactt			(Rat)	
NaV 1.3	(S)	agggaaggattgacttgcc	47°C	37	Y00766	295
	A	tggacctctccttagagtcca			(Rat)	
NaV 1.6	(S)	cgagagctatctggagaacggcca	55°C	30	NM_019266	440
	(A)	gcctcctcctgctgcttctt			(Rat)	
Kir 6.2	(S)	caccctgcgccatggccgcc	53°C	30	NM_031358	173
	(A)	ttaccacccacaccgttctc			(Rat)	
SUR 1	(S)	taytggtggatgaaygcctt	53°C	33	AB052294	752
	(A)	cttrgtrcsacraartactg			(Rat)	
TREK-1	(S)	tcaagcacatagaaggctgg	55°C	33	AF325671	434
	(A)	tcaggtggttcacagacagg			(Rat)	
TRAAK	(S)	gggcagcgccttcttttttct	55°C	32	AF302842	440
	(A)	ccagaaccacaccagcggct			(Rat)	
18S-rRNA	(S)	tcaagaacgaaagtcggagg	54°C	17	BK000964	494
	(A)	ggacatctaagggcatcaca			(Mouse)	

S, sense; A, antisense. For all of the reactions, preliminary experiments were performed to determine the number of PCR cycles at which saturation occurred. The experiments were carried out with the number of cycles that precedes saturation as indicated in the table.

made by unpaired *t* test. A difference was considered significant when the *P* value was less than 0.05 (Zar, 1984).

Results

The 10 fetal llamas had a mean weight of 4.07 ± 0.35 kg (mean ± S.E.M.) This weight corresponds to $71 \pm 2\%$ of gestation, gestational age $\sim 342 \pm 4$ days, where term weight is 10.3 ± 0.3 kg (Herrera *et al.* 2002).

Effects of prolonged hypoxaemia on maternal and fetal cardiorespiratory variables

In the hypoxaemic group, maternal P_{a,O_2} decreased from 92.5 ± 1.5 to 66.4 ± 7.8 mmHg ($P < 0.05$), whilst P_{a,CO_2} remained constant. Maternal haemoglobin saturation decreased from 95.0 ± 0.4 to $91.3 \pm 1.7\%$. No significant changes in maternal pH were observed. In the normoxaemic group, all these variables remained without significant changes during the study. Maternal heart rate and mean arterial blood pressure were not different between both groups, showing values of 54 ± 3 beats min^{-1} and 101 ± 10 mmHg, respectively, for normoxaemic group, and 60 ± 4 beats min^{-1} and 128 ± 16 mmHg, respectively, for hypoxaemic group

During prolonged hypoxaemia, there was a reduction in fetal P_{a,O_2} and haemoglobin saturation. No significant changes in fetal pH and P_{a,CO_2} were observed (Table 2). There were no significant effects of prolonged hypoxaemia on fetal mean heart rate and mean arterial pressure: 113 ± 4 beats min^{-1} and 43 ± 3 mmHg, respectively, in the normoxaemic group and 121 ± 4 beats min^{-1} and 41 ± 2 mmHg, respectively, in the hypoxaemic group.

Effects of prolonged hypoxaemia on fetal brain cortex and core temperature

We assessed effects of hypoxaemia by comparing absolute values of brain and core temperatures in normoxaemic and hypoxaemic fetuses (Fig. 1*A* and *B*) and by comparing differences in brain temperature minus core temperature over 24 h for each group of fetuses (Fig. 2*A* and *B*). Hypoxaemia had no effect on fetal brain cortex temperature during the first 14 h of hypoxaemia, when the brain temperatures of the hypoxaemic and the normoxaemic group were compared. Thereafter, from 15 h of hypoxaemia to the end of the experiment, brain temperature became significantly lower in the hypoxaemic group than the normoxaemic group (Fig. 1*A*; $P < 0.05$). Nevertheless, when the brain temperature of the hypoxaemic fetuses was compared with its basal temperature, it became significantly different at hour 4 and from 14 h onwards (Fig. 1*A*; $P < 0.05$). Absolute mean brain temperature decreased 0.54°C, from 38.83 ± 0.14°C in normoxaemia to 38.29 ± 0.17°C during prolonged

Table 2. pH and arterial blood gases in the fetal llama during 24 h of hypoxaemia

		Basal	4 h	8 h	12 h	16 h	20 h	24 h
pH	N	7.37 ± 0.02	7.36 ± 0.01	7.35 ± 0.01	7.35 ± 0.01	7.34 ± 0.01	7.35 ± 0.01	7.34 ± 0.01
	H	7.31 ± 0.01	7.32 ± 0.01	7.31 ± 0.01	7.32 ± 0.01	7.32 ± 0.01	7.31 ± 0.02	7.30 ± 0.02
P_{a,CO_2}	N	50 ± 2	49 ± 2	49 ± 2	47 ± 3	49 ± 3	48 ± 3	47 ± 3
(mmHg)	H	48 ± 2	44 ± 1	45 ± 2	45 ± 2	44 ± 1	45 ± 2	45 ± 2
P_{a,O_2}	N	18.2 ± 1.2	17.6 ± 1.2	18.5 ± 0.8	17.6 ± 0.7	18.8 ± 1.0	19.9 ± 0.9	18.0 ± 1.1
(mmHg)	H	17.7 ± 1.4	13.0 ± 0.4*	13.0 ± 0.4*	12.3 ± 0.5*	12.8 ± 0.5*	12.3 ± 0.5*	11.9 ± 0.8*
Hb	N	11.6 ± 0.4	12.1 ± 0.4	11.7 ± 0.6	11.2 ± 0.7	11.6 ± 0.6	11.1 ± 0.7	11.1 ± 0.5
(g dl^{-1})	H	10.3 ± 0.6	10.2 ± 0.7*	9.9 ± 0.7	9.7 ± 0.6	9.8 ± 0.5	9.5 ± 0.5	9.3 ± 0.6*
Sat Hb	N	44.6 ± 1.8	41.1 ± 1.8	45.0 ± 2.8	42.6 ± 2.4	43.7 ± 3.5	48.3 ± 3.3	41.2 ± 3.9
(%)	H	40.9 ± 4.8	26.3 ± 1.4*	24.9 ± 1.4*	24.7 ± 1.6*	24.9 ± 1.7*	23.5 ± 1.5*	21.2 ± 1.9*
O_2 cont	N	7.0 ± 0.3	6.8 ± 0.3	7.2 ± 0.5	6.5 ± 0.4	7.3 ± 0.3	7.8 ± 0.6	6.5 ± 0.4
((ml O_2) dl^{-1})	H	5.8 ± 0.7	3.8 ± 0.3*	3.4 ± 0.3*	3.4 ± 0.3*	3.4 ± 0.3*	3.2 ± 0.3*	2.8 ± 0.3*

P_{a,CO_2}, arterial partial pressure of carbon dioxide; P_{a,O_2} arterial partial pressure of oxygen; Hb, haemoglobin; Sat Hb, percentage saturation of Hb; O_2 cont, oxygen content. Values are shown as means ± S.E.M.; $n = 5$. *$P < 0.05$, one way ANOVA for repeated measures and Newman-Keuls test. Normoxaemia (N) *versus* hypoxaemia (H).

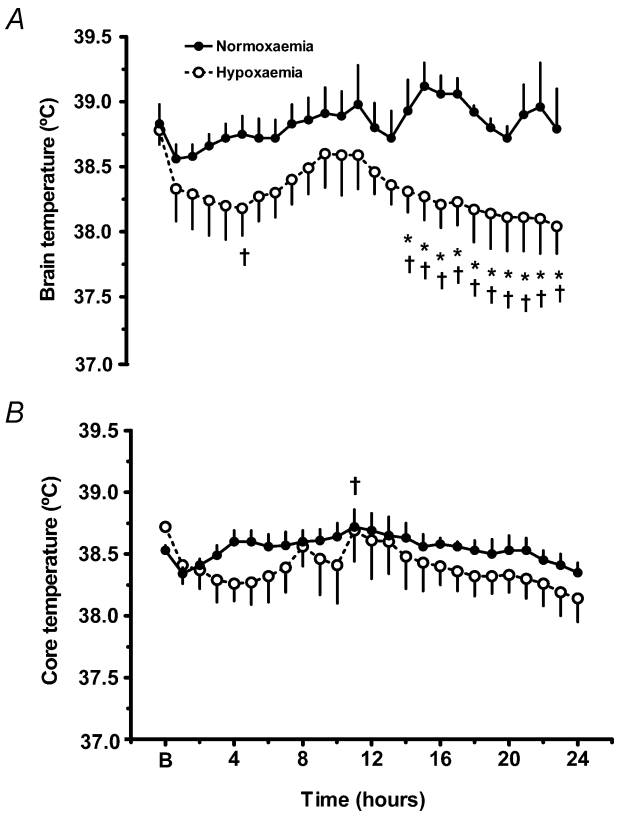

Figure 1. Cerebral and core temperature in fetal llama during 24 h of hypoxaemia
Brain cortex (*A*) and core (*B*) temperatures. Values are expressed as means ± S.E.M.; $n = 5$ for each group. B is the mean basal temperature obtained during 1 h before starting the hypoxaemia. *A*, Normoxaemia (●) *versus* hypoxaemia (○), *$P < 0.05$, two-way ANOVA for repeated measures and Newman-Keuls test. Hour 4 and hours 15–24 of hypoxaemia *versus* basal, †$P < 0.05$, one-way ANOVA for repeated measures and Newman-Keuls test. *B*, hour 1 *versus* hour 11, †$P < 0.05$, one-way ANOVA for repeated measures and Newman-Keuls test.

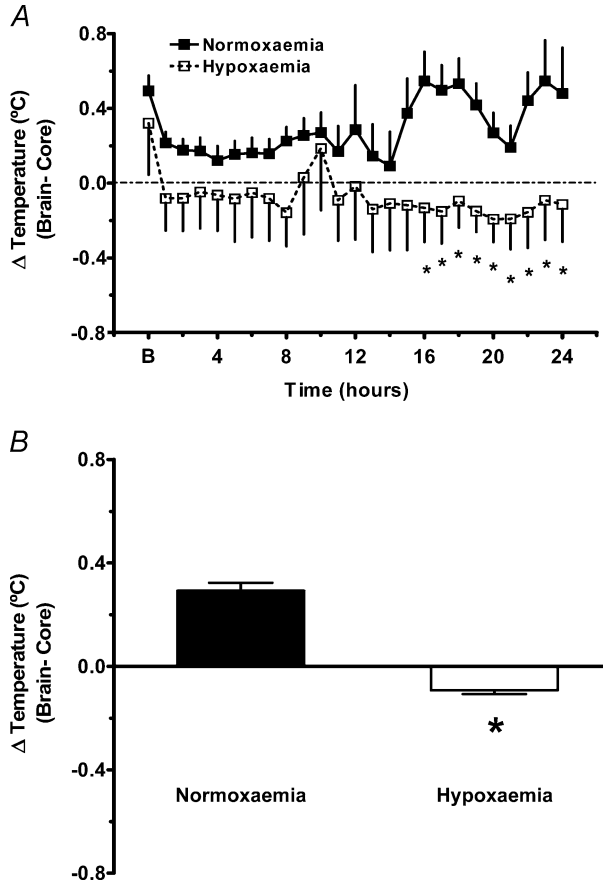

Figure 2. Cerebral and core temperature difference in fetal llama during 24 h of hypoxaemia
Brain cortex temperature minus core temperature (*A*) and brain cortex temperature minus core temperature as an average of 24 h measurements (*B*). Values are expressed as means ± S.E.M.; $n = 5$ for each group. B is the mean basal temperature obtained during 1 h before starting the hypoxaemia. *A*, normoxaemia (■) *versus* hypoxaemia (□), *$P < 0.05$, two-way ANOVA for repeated measures and Newman-Keuls test. *B*, normoxaemia (filled bars) *versus* hypoxaemia (open bars), *$P < 0.001$, unpaired Student's *t* test.

hypoxaemia. In contrast, in the normoxaemic group, there were no significant changes in brain temperature when compared with the basal value. This fall in temperature in the hypoxaemic group was restricted to the brain, as there were no significant differences in fetal core temperature between normoxaemic and hypoxaemic fetuses during the 24 h recorded (Fig. 1*B*). However, a significant circadian variation was observed in the core temperature in the normoxaemic fetuses (Fig. 1*B*; $P < 0.05$).

The brain cortex temperature minus core temperature difference was statistically significant between normoxaemic and hypoxaemic fetuses from the 16th hour of hypoxaemia until the end of the study period (Fig. 2*A*; $P < 0.05$). When the average of the brain temperature minus core temperature difference was calculated, there was a significant difference between normoxaemic and hypoxaemic fetuses (Fig. 2*B*; $P < 0.001$). This difference was below zero in the hypoxaemic fetuses, whilst it was above zero in the normoxaemic fetuses (Fig. 2*B*).

Effects of prolonged hypoxaemia on Na^+–K^+-ATPase activity and ouabain binding in the brain cortex

The Na^+–K^+-ATPase activity in the brain cortex of hypoxaemic fetuses was reduced to about 50% of the normoxaemic fetuses (Fig. 3*A*; $P < 0.05$). Consistent with this lower activity, ouabain B_{MAX} was about 30% lower in the hypoxaemic fetal brain cortex than in the normoxaemic fetal brain cortex (Fig. 3*B* and *C*; $P < 0.05$), whilst K_D for this inhibitor was unaffected (12.7 ± 0.9 nM for normoxaemia, and 11.5 ± 1.0 nM for hypoxaemia)

Effects of prolonged hypoxaemia on the expression of Na^+ and K^+ channels

We determined whether Na^+–K^+-ATPase reduction in the fetal brain cortex was coupled with a reduction of the expression of some Na^+ and K^+ channels. We did observe a significant decrease of the NaV1.1 protein channel detected by immunoblot in the brain of the hypoxaemic group (Fig. 4; $P < 0.05$). We also detected a decrease on the NaV1.2 channel protein in this group, although the difference did not reach statistical significance (Fig. 4; $P = 0.075$). NaV1.3 protein abundance was not different between the two groups, while NaV1.6 protein was not detected by the antibody (data not shown). We did not see any difference in the amounts of NaV1.1, NaV1.2, NaV1.3 and NaV1.6 transcripts measured by semiquantitative RT-PCR (data not shown).

Moreover, we did not observe differences between normoxaemic and hypoxaemic fetal llamas in the expression of the following K^+ channels: K_{ATP} channel assessed by glybenclamide binding and by semi-quantitative RT-PCR of Kir6.2 and SUR1 subunits, and TREK1 and TRAAK channels, which were also measured by semiquantitative RT-PCR (data not shown).

Effects of prolonged hypoxaemia on PARP proteolysis

The increased degradation of poly ADP-ribose polymerase (PARP) from its intact form of 113 kDa into proteolytic

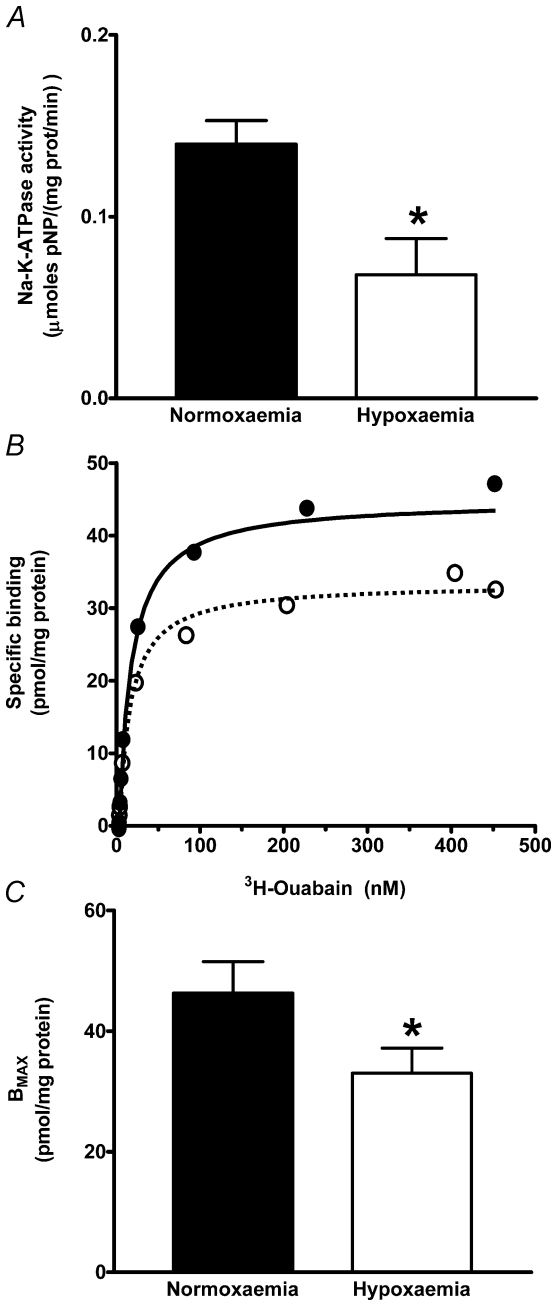

Figure 3. Na^+–K^+-ATPase in fetal llama brain cortex submitted to 24 h of hypoxaemia
A, Na^+–K^+-ATPase activity; *B*, representative ouabain binding saturation curves; *C*, calculated maximal binding (B_{MAX}). Values are expressed as means ± S.E.M.; $n = 5$ for each group; $^*P < 0.05$, unpaired Student's *t* test. Normoxaemia (filled bars, ●) *versus* hypoxaemia (open bars, ○).

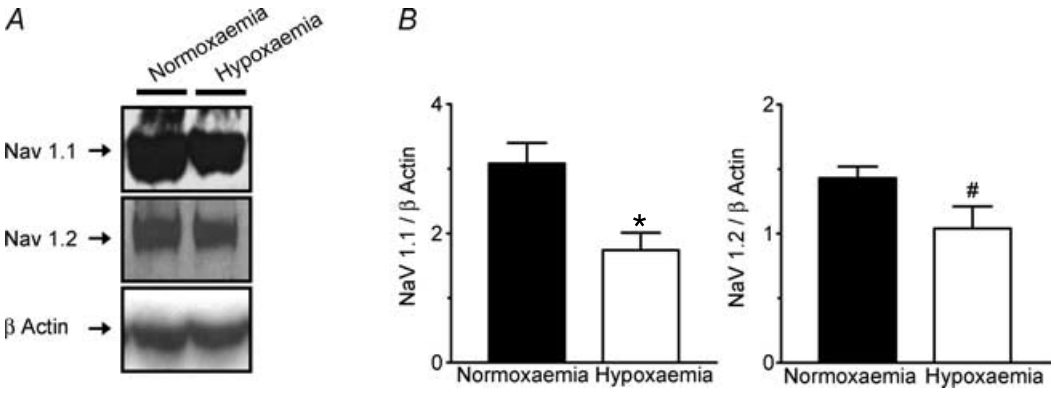

Figure 4. NaV 1.1 and NaV 1.2 channel immunoblot detection in fetal llama brain submitted to 24 h of hypoxaemia
Representative immunoblot (*A*) and semiquantitative analysis (*B*) of NaV 1.1 and NaV 1.2 in brain cortex from fetal llama. Values are expressed as means ± S.E.M.; $n = 5$ for each group; $^*P < 0.05$, $\#P = 0.075$, unpaired Student's *t* test. Normoxaemia (filled bars) *versus* hypoxaemia (open bars).

fragments of 85 and 29 kDa is a good marker of increased apoptosis in a given experimental condition (Sallmann *et al.* 1997). PARP can be also degraded during necrosis into major proteolytic fragments of 50–55 kDa and 62 kDa. Since our antibody recognizes the intact form, its apoptotic 85 kDa fragment and its necrotic 62 kDa fragment, both apoptosis and necrosis, can be assessed (Gobeil *et al.* 2001). We measured the ratio between the 85 kDa apoptotic fragment and the intact form of PARP in the fetal brain cortex, and we did not detect a significant difference in this ratio between normoxaemic and hypoxaemic fetal llamas (Fig. 5), suggesting that 24 h hypoxaemia did not stimulate brain cell apoptosis. We did not detect the necrotic 62 kDa fragment in any of the animals studied, suggesting the absence of necrosis during prolonged hypoxaemia.

Discussion

This study provides further evidence to support the hypothesis that the fetal llama responds to prolonged hypoxaemia with brain hypometabolism, and we examined some of the possible mechanisms involved. We found a decrease in brain cortex temperature during prolonged hypoxaemia, which was accompanied by a decrease in brain cortex Na^+–K^+-ATPase activity, and by decrease in NaV1.1 and NaV1.2 channel proteins. These changes occurred in the absence of changes in PARP protein degradation, suggesting that cell death of the brain was not enhanced in the fetal llama during hypoxaemia. Taken together, all these results support the view that some strategies may have evolved in the fetal llama to avoid hypoxic cerebral damage, and that these are imposed by the sustained oxygen shortage in life at extreme altitude.

Prolonged hypoxaemia resulted in a drop in fetal brain cortex temperature assessed as absolute brain cortex temperature *versus* normoxaemic fetuses and *versus* their own basal values. The fetal brain produces heat as a consequence of its metabolic processes, which include Na^+–K^+-ATPase activity. Brain temperature is a function of the heat production derived from oxygen consumption, heat loss and the specific heat of the tissue. About 4.8 cal (20.08 J) are produced per millilitre of oxygen used, an equivalency that varies less than 11%, irrespective of whether the substrate is glucose, fat or protein (Carpenter *et al.* 1939; Hunter *et al.* 2003). Heat leaves the fetal brain mainly by diffusing into the blood perfusing the brain, and a negligible amount is transferred across

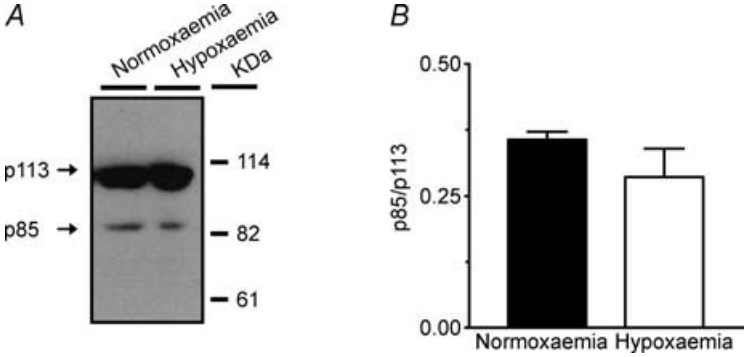

Figure 5. Immunoblot detection of poly ADP-ribose polymerase (PARP) in fetal llama brain submitted to 24 h of hypoxaemia
Representative immunoblot detection (*A*) and semiquantitative analysis (*B*) of intact (p113) and proteolytic fragment (p85) in the brain cortex of fetal llama. Values are expressed as means ± S.E.M.; $n = 5$ for each group. Normoxaemia (filled bar) *versus* hypoxaemia (open bar).

the fetal dura, bone and skin to the amniotic and allantoic fluids (Hunter *et al.* 2003). Our experiments show that absolute mean brain temperature decreased 0.54°C during prolonged hypoxaemia, indicating lower heat production or an increase in release of heat from the brain. Previous findings show a lowering of brain cortex oxygen consumption in an episode of acute hypoxaemia (1 h) in the llama fetus (Llanos *et al.* 2002), suggesting that a reduction in heat production (beyond the scope of the present study) is probably present during the first hour of hypoxaemia. A reduction in brain heat production has been shown by Hunter *et al.* (2003) in an episode of 30 min hypoxaemia in fetal sheep. Fetal llama brain temperature significantly decreased at 4 h and then 15 h thereafter of hypoxaemia. Acute hypoxaemia does not increase brain blood flow in the fetal llama (Llanos *et al.* 2002). Therefore, we assume a constant inflow and removal of heat by the blood that will require time to be detected as a significant temperature change. In fetal lambs asphyxia also decreases brain heat production; in addition, it reduces oxygen consumption, and brain temperature (Hunter *et al.* 2003). In adult cats, focal brain ischaemia induced by occluding the left middle cerebral artery decreased temperature in the ischaemic brain tissue (Zauner *et al.* 1995).

The brain temperature of the fetal sheep in normoxaemic conditions is higher than of the incoming blood (carotid artery) (Hunter *et al.* 2003). A similar observation was obtained when brain minus right atrium temperature were measured in the normoxaemic llama fetus. The mean difference was 0.29 ± 0.03°C. In this study, we considered the temperature in the right atrium as core temperature. The right atrium in the fetal sheep receives 65% of the combined ventricular output (CVO), collecting 60% of inferior vena cava return (40% of the CVO), 100% of the superior vena cava return (22% of the CVO) and 100% of the coronary sinus return (3% of the CVO) (Teitel *et al.* 1987). Therefore, the temperature in the right atrium can be regarded as a good indicator of core temperature. It is likely that the temperature of the right atrium is higher than the carotid artery, since the left atrium receives preferentially cooler blood coming from the umbilical vein (Reuss *et al.* 1981). If we had used carotid temperature instead of right atrial temperature, the brain minus core temperature in normoxaemic and hypoxaemic fetuses would most likely have been higher.

A significant circadian variation was observed in the core temperature in the normoxaemic llama fetuses, oscillation also shown by Laburn *et al.* (1992) in fetal sheep. The core temperature of hypoxaemic fetuses did not show a statistically significant circadian variation. This lack of significant variation was also noted in the brain temperatures. Nevertheless, assessment of circadian variations was not a purpose of this paper, as we left the room lights on during the whole procedure.

Hypoxaemia resulted in a marked decrease in the difference between brain and core temperature. Nevertheless, we did not observe a decrease in core temperature during the episode of prolonged hypoxaemia. We found that most values of brain minus core temperature in hypoxaemic fetuses became negative, in marked contrast with the observation in normoxaemic fetuses. In addition, the average of the brain minus core temperature was significantly lower in hypoxaemic than normoxaemic fetuses, an observation consistent with a decrease in brain metabolic activity during hypoxaemia. A decrease in fetal brain metabolic activity during episodes of acute hypoxaemia or asphyxia has also been found by Hunter *et al.* (2003) and Kubonoya *et al.* (1998).

Our data suggest that the lower temperature registered in the brain cortex from the hypoxaemic fetal llamas, could be the result of decreased Na^+–K^+-ATPase activity. In hypoxaemic fetal llamas, brain Na^+–K^+-ATPase activity was about half that of normoxaemic fetuses. Other authors have also reported a reduction of this enzyme as a result of hypoxia or hypoxia/ischaemia in the brain. Hypoxia or hypoxia/ischaemia decreases brain Na^+–K^+-ATPase activity in newborn lambs and piglets and in preterm guinea pigs fetuses. These authors interpreted the reduction of Na^+–K^+-ATPase activity as damage in the enzyme produced by reactive oxygen species and as sign of brain damage (Groenendaal *et al.* 2000; Rosenkrantz *et al.* 1996; and Graham *et al.* 1995). Alternatively in the anoxic turtle, the reduced Na^+–K^+-ATPase activity without cell depolarization observed in hepatocytes, or the reversible inhibition of Na^+–K^+-ATPase activity measured in telencephalon and cerebellum, has been considered as part of the channel arrest mechanism to adapt the metabolism to oxygen lack (Buck & Hochachka, 1993; Hylland *et al.* 1997). Moreover, in the anoxic turtle, the Na^+–K^+-ATPase activity remains unchanged in the brain stem, responsible for cardiovascular control, suggesting the need to preserve the metabolism in this territory (Hylland *et al.* 1997). In agreement with these findings, we did not detect changes of Na^+–K^+-ATPase activity in the brain stem from hypoxaemic llama fetus (Reyes, unpublished results). These results support the idea that the reduction of this enzymatic activity in the brain cortex is an adaptive response restricted to some areas of the brain, rather than a generalized physiopathological change.

Hypoxic brain damage (cell death) is manifested as apoptosis, necrosis or both. Apoptosis can be promoted by ischaemia, by oxygen and glucose deprivation or by hypoxia alone (Guégan & Sola, 2000; Wei *et al.* 2003; Daval *et al.* 2004). Necrosis occurs in the core of severe hypoxic/ischaemic lesions, whereas apoptosis takes place in the periphery of those lesions, where hypoxia is moderate or less extreme (Friedlander, 2003). Biochemical and cellular changes in cell death indicators are detected in intervals

between 1 h to 24 h after the onset of the injury, even when the cell death process may extend beyond this period. These changes were observed after the exposure to acute hypoxia in cultured fetal rat brain neurones or in brain cortex from newborn rats (Bossenmeyer-Pourié *et al.* 2002; Hu *et al.* 2003); they were also found following an episode of hypoxia/ischaemia in brain cortex from fetal, newborn or adult rats or mice (De Torres *et al.* 1997; Guégan & Sola, 2000; Benchoua *et al.* 2001; Calvert *et al.* 2003; Robinson *et al.* 2005). We investigated whether prolonged hypoxaemia resulted in apoptosis and or necrosis in the brain of the llama fetus by measuring PARP proteolysis. PARP is an enzyme involved in DNA repair processes, and it is a substrate for caspases 3 and 7, which degrade the 113 kDa intact form of PARP into 85 kDa and 29 kDa fragments. Activation of the caspase cascade by apoptosis inducers leads to an increase of the proteolytic fragments relative to the intact form (Guégan & Sola, 2000; Jayanthi *et al.* 2004). Necrosis inducers also promote PARP degradation yielding different fragments, including proteolytic bands of 50–55 kDa and a 62 kDa band corresponding to the N-terminal portion of PARP (Gobeil *et al.* 2001). In the fetal llama brain cortex, we found that the ratio of the 85 kDa proteolytic fragment of PARP to the 113 kDa intact form of the enzyme was not changed by prolonged hypoxaemia. Neither in hypoxaemia nor in normoxaemia did we detected PARP fragments attributable to necrosis. Moreover, in preliminary experiments we did not observe increases in apoptotic degradation of caspase-9 precursor as a result of hypoxaemia in the fetal llama brain cortex (R. V. Reyes, unpublished results). The latter reinforces the idea that in hypoxaemic fetal llamas there was no increase in neuronal death.

In contrast to the studies in other species, in which Na^+–K^+-ATPase decrease was interpreted as brain damage, our results show that decrease in the brain Na^+–K^+-ATPase activity induced by prolonged hypoxaemia in the fetal llama is not accompanied by an increase in cell death, suggesting that we are looking an adaptive response.

Several mechanisms may lead to decreases in the amount or in the activity of Na^+–K^+-ATPase. This enzyme is a heterodimer formed by one α subunit and one β subunit. The α subunit is responsible for the catalytic activity and binds the inhibitor ouabain (Blanco & Mercer, 1998). The decrease in Na^+–K^+-ATPase activity found in the fetal llama during hypoxaemia could be explained, at least in part, by diminished α subunit content in the cortex membranes, as implied by the lower ouabain binding. B_{MAX} for ouabain decreased about 30% compared with normoxaemic controls, whilst K_D was unchanged. A reduction in the number of molecules of Na^+–K^+-ATPase at the membrane can be accomplished either by changes of gene expression, or by endocytosis and translocation of the α subunits from the membrane to intracellular compartments. These mechanisms have been described in the response to a variety of hormones and neurotransmitters, such as insulin, thyroid hormone and catecholamines, among others (Ewart & Klip, 1995; Beron *et al.* 1997; Chibalin *et al.* 1999; Banerjee & Chaudhury, 2002; Bertorello *et al.* 2003; Al-Khalili *et al.* 2004). Direct modulation of Na^+–K^+-ATPase activity through phosphorylation/dephosphorylation has been described for the three catalytic α subunits ($\alpha1$, $\alpha2$ and $\alpha3$) found in nervous cells, including the predominant $\alpha3$ subunit (Ewart & Klip, 1995; Blanco & Mercer, 1998; Nishi *et al.* 1999). The presence of endogenous inhibitors of the Na^+ pump in biological fluids and tissues has been described (Rodríguez de Lores Arnaiz, 2000). Moreover, hypoxia induces the release of one of these inhibitors from the adrenal glands (De Angelis & Haupert, 1998). Whether one or more of these mechanisms contribute to decrease cerebral cortex Na^+–K^+-ATPase in the fetal llama during hypoxaemia deserves further investigation.

A decrease in Na^+–K^+-ATPase activity during hypoxia could be an adaptive mechanism in some species. A reduction of Na^+–K^+-ATPase activity should result in strong ATP savings, given that more than 50% of ATP produced by the neurone is utilized by Na^+–K^+-ATPase to maintain the electrochemical gradient over the cell membrane, supporting the repetitive opening and closure of ion channels (Erecinska & Silver, 1994). However, to avoid cell membrane depolarization and concurrent brain damage, decreased Na^+–K^+-ATPase activity should be coupled to decreases in Na^+ and K^+ permeability in the cell membrane. The diminution of ion channel permeability can occur as the result of a fall in channel activity or as the result of drop in the number of channel proteins at the membrane, as described for the anoxic turtles. We investigated whether the observed reduction of Na^+–K^+-ATPase activity by hypoxaemia in the fetal llama brain was accompanied by a reduction of the expression of Na^+ and K^+ channels. Therefore, we measured protein and mRNA levels of voltage-dependent sodium channels (NaV channels), and the expression of K_{ATP} channels, which sense the intracellular ATP levels (Ashcroft & Gribble, 1998), and the background potassium channels TREK1 and TRAAK (Fink *et al.* 1996, 1998; Patel & Honoré, 2001), which contribute to the baseline K^+ currents.

Of the nine α subunits of the NaV channels, we studied α subunits NaV1.1, NaV1.2, NaV1.3 and NaV1.6, expressed at the central nervous system (Novakovic *et al.* 2001). We found decreases in two of these channels. NaV1.1 protein was significantly decreased, whereas NaV1.2 showed a tendency to fall ($P = 0.075$), suggesting that reduction of the number of NaV1.1 and NaV1.2 molecules at the membrane could contribute to reduce ion permeability in the metabolically depressed fetal llama brain. Although hypoxaemia did not affect the protein

levels of NaV1.3, or the mRNA level of NaV1.3 and of NaV1.6, a potential contribution of these NaV channels by rapid and reversible inhibition cannot be discarded. Interestingly, we did not detect changes in the level of NaV1.1 or NaV1.2 mRNA transcripts in response to hypoxaemia, suggesting that translational regulation or post-translational modifications, rather than modulation of transcription, determine the NaV1.1 or NaV1.2 protein abundance. In fact, post-translational modifications, such as ubiquitination, enhance endocytosis and degradation, and have been proposed to be important in the regulation of the density of NaV channels in fetal brain neurones (Dargent *et al.* 1995; Paillart *et al.* 1996; Fotia *et al.* 2004; Rougier *et al.* 2005).

Reduction of neuronal excitability by diminution in the content of Na^+ channels has been reported as an adaptation to 24 h anoxia in the turtle brain (Pérez-Pinzón *et al.* 1992). Furthermore, inactivation of Na^+ currents has been reported in adult human cortical neurones and in murine young neurones from the hippocampus during the exposure to hypoxia (Cummins *et al.* 1993; Gu & Haddad, 2001). In the rats, the NaV channel expression response to prolonged hypoxia varies depending on the age; an increase in total NaV mRNA transcript and in protein expression is described for fetal brain. In contrast, a decrease in both transcript and protein is detected in the adult rat (Xia & Haddad, 1999). The difference between our results and the results described for fetal rats may represent species diversity.

We have already discussed a reduction in the expression of two NaV channels in the fetal llama brain cortex after 24 h of hypoxaemia. To have a functional ion channel arrest, there must be also a reduction in the K^+ permeability and/or expression of K^+ channels during hypoxaemia in the fetal llama brain. We did not find significant changes on the expression of K_{ATP} channels assessed by glybenclamide binding or by the transcript levels from both Kir6.2 and SUR1 subunits. The expression of K_{2P} family channels members TREK1 and TRAAK assessed by RT-PCR also remained unchanged. Despite these observations, we can not ignore a reduction of their activities by rapid mechanisms independent of gene expression, such as phosphorylation by protein kinase C and protein kinase A, which have an inhibitory action on TREK1 currents (Fink *et al.* 1996; Patel *et al.* 1998). On the other hand, more than 80 mammalian K^+ channel subunits have been identified to date; many of them with robust expression on the brain and with electrophysiological properties such as oxygen sensitivity that makes them good candidates to participate in the metabolic brain adaptation to hypoxia (Coetzee *et al.* 1999; Patel & Honoré, 2001). In the turtle brain, the K^+ leaking is reduced to 30–50% of normoxic levels between 1 and 2 h of anoxia in a rapid response principally mediated by adenosine receptors (Pék & Lutz, 1997; Pék-Scott & Lutz, 1998). For instance, the inhibition of the oxygen- and protein-kinase-A-inhibitable background K^+ channel TASK1 could participate in early reduction of passive K^+ permeability during anoxia (Buck, 2004). Moreover, the transcript levels of the Kv1 K^+ channel family reversibly drops to 20% of normoxic level in the course of 4 h of anoxia, suggesting a long-term adaptation in the strategy to reduce metabolic demands (Prentice *et al.* 2003). Further studies would address these possibilities in the llama fetus.

In summary, we have found that the fetal llama reacts to hypoxia with temperature reduction and a lowering of Na^+–K^+-ATPase activity and content in the brain cortex without signs of cell death. A decrease in the number of NaV1.1 and NaV1.2 channel molecules at the membrane may partially contribute to the ion permeability reduction needed to accomplish these changes without brain damage. These changes strongly support a condition of brain hypometabolism, which is an adaptive and effective mechanism to withstand hypoxia in the llama fetus.

References

Al-Khalili L, Kotova O, Tsuchida H, Ehren I, Feraille E, Krook A & Chibalin AV (2004). ERK1/2 mediates insulin stimulation of Na^+,K^+-ATPase by phosphorylation of the alpha-subunit in human skeletal muscle cells. *J Biol Chem* **279**, 25211–25218.

American Physiological Society (2002). Guiding principles for research involving animals and human beings. *Am J Physiol Regul Integr Comp Physiol* **283**, R281–283.

Ashcroft FM & Gribble FM (1998). Correlating structure and function in ATP-sensitive K^+ channels. *Trends Neurosci* **21**, 288–294.

Banerjee B & Chaudhury S (2002). Thyroidal regulation of different isoforms of Na^+,K^+-ATPase in the primary cultures of neurons derived from fetal rat brain. *Life Sci* **71**, 1643–1654.

Benavides CE, Pérez R, Espinoza M, Cabello G, Riquelme R, Parer JT & Llanos AJ (1989). Cardiorespiratory functions in the fetal llama. *Resp Physiol* **75**, 327–334.

Benchoua A, Guégan C, Couriaud C, Hosseini H, Sampaïo N, Morin D & Onténiente B (2001). Specific caspase pathways are activated in the two stages of cerebral infarction. *J Neurosci* **21**, 7127–7134.

Beron J, Forster I, Beguin P, Geering K & Verrey F (1997). Phorbol 12-myristate 13-acetate down-regulates Na^+,K^+-ATPase independent of its protein kinase C site: decrease in basolateral cell surface area. *Mol Biol Cell* **8**, 387–398.

Bertorello AM, Komarova Y, Smith K, Leibiger IB, Efendiev R, Pedemonte CH, Borisy G & Sznajder JI (2003). Analysis of Na^+,K^+-ATPase motion and incorporation into the plasma membrane in response to G protein-coupled receptor signals in living cells. *Mol Biol Cell* **14**, 1149–1157.

Bickler PE & Buck LT (1998). Adaptations of vertebrate neurons to hypoxia and anoxia: maintaining critical Ca^{2+} concentrations. *J Exp Biol* **201**, 1141–1152.

Blanco G & Mercer RW (1998). Isozymes of the Na^+,K^+-ATPase: heterogeneity in structure, diversity in function. *Am J Physiol Renal Physiol* **275**, F633–650.

Bossenmeyer-Pourié C, Lievre V, Grojean S, Koziel V, Pillot T & Daval JL (2002). Sequential expression patterns of apoptosis- and cell cycle-related proteins in neuronal response to severe or mild transient hypoxia. *Neuroscience* **114**, 869–882.

Buck LT (2004). Adenosine as a signal for ion channel arrest in anoxia-tolerant organisms. *Comp Biochem Physiol B Biochem Mol Biol* **139**, 401–414.

Buck LT & Hochachka PW (1993). Anoxic suppression of Na^+–K^+-ATPase and constant membrane potential in hepatocytes: support for channel arrest. *Am J Physiol Regul Integr Physiol* **265**, R1020–1025.

Calvert JW, Zou C, Nanda A & Zhang JH (2003). Effect of hyperbaric oxygen on apoptosis in neonatal hypoxia-ischemia rat model. *J Appl Physiol* **95**, 2072–2080.

Carpenter TM (1939). *Tables for Respiratory Exchange*. Carnegie Institution of Washington, Washington.

Chibalin AV, Ogimoto G, Pedemonte CH, Pressley TA, Katz AI, Feraille E, Berggren PO & Bertorello AM (1999). Dopamine-induced endocytosis of Na^+,K^+-ATPase is initiated by phosphorylation of Ser-18 in the rat alpha subunit and is responsible for the decreased activity in epithelial cells. *J Biol Chem* **274**, 1920–1927.

Coetzee WA, Amarillo Y, Chiu J, Chow A, Lau D, McCormack T, Moreno H, Nadal MS, Ozaita A, Pountney D, Saganich M, Vega-Saenz de Miera E & Rudy B (1999). Molecular diversity of K^+ channels. *Ann N Y Acad Sci* **868**, 233–285.

Cummins TR, Jiang C & Haddad GG (1993). Human neocortical excitability is decreased during anoxia via sodium channel modulation. *J Clin Invest* **91**, 608–615.

Dargent B, Jullien F & Couraud F (1995). Internalization of voltage-dependent sodium channels in fetal rat brain neurons: a study of the regulation of endocytosis. *J Neurochem* **65**, 407–413.

Daval JL, Pourie G, Grojean S, Lievre V, Strazielle C, Blaise S & Vert P (2004). Neonatal hypoxia triggers transient apoptosis followed by neurogenesis in the rat CA1 hippocampus. *Pediatr Res* **55**, 561–567.

De Angelis C & Haupert GT Jr (1998). Hypoxia triggers release of an endogenous inhibitor of Na^+–K^+-ATPase from midbrain and adrenal. *Am J Physiol Renal Physiol* **274**, F182–188.

De Torres C, Munell F, Ferrer I, Reventós J & Macaya A (1997). Identification of necrotic cell death by the TUNEL assay in the hypoxic-ischemic neonatal rat brain. *Neurosci Lett* **230**, 1–4.

Erecinska M & Silver IA (1994). Ions and energy in mammalian brain. *Prog Neurobiol* **43**, 37–71.

Ewart HS & Klip A (1995). Hormonal regulation of the Na^+–K^+-ATPase: mechanisms underlying rapid and sustained changes in pump activity. *Am J Physiol Cell Physiol* **269**, C295–311.

Fink M, Duprat F, Lesage F, Reyes R, Romey G, Heurteaux C & Lazdunski M (1996). Cloning, functional expression and brain localization of a novel unconventional outward rectifier K^+ channel. *EMBO J* **15**, 6854–6862.

Fink M, Lesage F, Duprat F, Heurteaux C, Reyes R, Fosset M & Lazdunski M (1998). A neuronal two P domain K^+ channel stimulated by arachidonic acid and polyunsaturated fatty acids. *EMBO J* **17**, 3297–3308.

Fotia AB, Ekberg J, Adams DJ, Cook DI, Poronnik P & Kumar S (2004). Regulation of neuronal voltage-gated sodium channels by the ubiquitin-protein-ligases Nedd4 and Nedd4-2. *J Biol Chem* **279**, 28930–28935.

Friedlander RM (2003). Apoptosis and caspases in neurodegenerative diseases. *N Engl J Med* **348**, 1365–1375.

Giussani DA, Riquelme RA, McGarrigle HHG, Moraga FA, Gaete CR, Sanhueza EM, Hanson MA & Llanos AJ (1996). Chemoreflex and endocrine components of cardiovascular responses to acute hypoxemia in the llama fetus. *Am J Physiol Regul Integr Comp Physiol* **271**, R73–83.

Gobeil S, Boucher CC, Nadeau D & Poirier GG (2001). Characterization of the necrotic cleavage of poly (ADP-ribose) polymerase (PARP-1): implication of lysosomal proteases. *Cell Death Differ* **8**, 588–594.

Graham E, Mishra OP & Delivoria-Papadopoulos M (1995). Effect of *in utero* hypoxia on the ouabain/strophanthidin binding site of the fetal guinea pig brain cell membrane Na^+,K^+-ATPase. *Neurosci Lett* **185**, 159–162.

Groenendaal F, Shadid M, McGowan JE, Mishra OP & van Bel F (2000). Effects of deferoxamine, a chelator of free iron, on Na^+,K^+-ATPase activity of cortical brain cell membrane during early reperfusion after hypoxia-ischemia in newborn lambs. *Pediatr Res* **48**, 560–564.

Gu XQ & Haddad GG (2001). Decreased neuronal excitability in hippocampal neurons of mice exposed to cyclic hypoxia. *J Appl Physiol* **91**, 1245–1250.

Guégan C & Sola B (2000). Early and sequential recruitment of apoptotic effectors after focal permanent ischemia in mice. *Brain Res* **856**, 93–100.

Harris P, Heath D, Smith P, Williams DR, Ramirez A, Kruger H & Jones DM (1982). Pulmonary circulation of the llama at high and low altitudes. *Thorax* **37**, 38–45.

Herrera EA, Riquelme RA, Sanhueza EM, Raggi LA & Llanos AJ (2002). Use of fetal biometry to determine fetal age in late pregnancy in llamas. *Anim Reprod Sci* **74**, 101–109.

Hu X, Qiu J, Grafe MR, Rea HC, Rassin DK & Perez-Polo JR (2003). Bcl-2 family members make different contributions to cell death in hypoxia and/or hyperoxia in rat cerebral cortex. *Int J Dev Neurosci* **21**, 371–377.

Hunter CJ, Blood AB & Power GG (2003). Cerebral metabolism during cord occlusion and hypoxia in the fetal sheep: a novel method of continuous measurement based on heat production. *J Physiol* **552**, 241–251.

Hylland P, Milton S, Pék M, Nilsson GE & Lutz PL (1997). Brain Na^+–K^+-ATPase activity in two anoxia tolerant vertebrates: crucian carp and freshwater turtle. *Neurosci Lett* **235**, 89–92.

Jayanthi S, Deng X, Noailles P-AH, Ladenheim B & Cadet JL (2004). Methamphetamine induces neuronal apoptosis via cross-talk between endoplasmic reticulum and mitochondria-dependent death cascades. *FASEB J* **18**, 238–251.

Kubonoya K, Yoneyama Y, Sawa R, Araki T & Power GG (1998). Brain temperature and metabolic responses during umbilical cord occlusion in fetal sheep. *Pflugers Arch* **436**, 667–672.

Laburn HP, Mitchell D & Goelst K (1992). Fetal and maternal body temperatures measured by radiotelemetry in near-term sheep during thermal stress. *J Appl Physiol* **72**, 894–900.

Llanos AJ, Riquelme RA, Moraga FA, Cabello G & Parer JT (1995). Cardiovascular responses to graded of hypoxaemia in the llama fetus. *Reprod Fertil Dev* **7**, 549–552.

Llanos AJ, Riquelme RA, Sanhueza EM, Hanson MA, Blanco CE, Parer JT, Herrera EA, Pulgar VM, Reyes RV, Cabello G & Giussani DA (2003). The fetal llama versus the fetal sheep: different strategies to withstand hypoxia. *High Alt Med Biol* **4**, 193–202.

Llanos AJ, Riquelme RA, Sanhueza EM, Herrera EA, Cabello G, Giussani DA & Parer JT (2002). Regional brain blood flow and cerebral hemispheric oxygen consumption during acute hypoxaemia in the llama fetus. *J Physiol* **538**, 975–983.

Moraga FA, Monge C, Riquelme RA & Llanos AJ (1996). Fetal and maternal blood oxygen affinity: a comparative study in llamas and sheep. *Comp Biochem Physiol* **115A**, 111–115.

Nilsson GE & Lutz PL (2004). Anoxia tolerant brains. *J Cereb Blood Flow Metab* **24**, 475–486.

Nishi A, Fisone G, Snyder GL, Dulubova I, Aperia A, Nairn AC & Greengard P (1999). Regulation of Na^+,K^+-ATPase isoforms in rat neostriatum by dopamine and protein kinase C. *J Neurochem* **73**, 1492–1501.

Novakovic SD, Eglen RM & Hunter JC (2001). Regulation of Na^+ channel distribution in the nervous system. *Trends Neurosci* **24**, 473–478.

Paillart C, Boudier JL, Boudier JA, Rochat H, Couraud F & Dargent B (1996). Activity-induced internalization and rapid degradation of sodium channels in cultured fetal neurons. *J Cell Biol* **134**, 499–509.

Patel AJ & Honoré E (2001). Molecular physiology of oxygen-sensitive potassium channels. *Eur Respir J* **18**, 221–227.

Patel AJ, Honoré E, Maingret F, Lesage F, Fink M, Duprat F & Lazdunski M (1998). A mammalian two pore domain mechano-gated S-like K^+ channel. *EMBO J* **17**, 4283–4290.

Pék M & Lutz PL (1997). Role for adenosine in channel arrest in the anoxic turtle brain. *J Exp Biol* **200**, 1913–1917.

Pék-Scott M & Lutz PL (1998). ATP-sensitive K^+ channel activation provides transient protection to the anoxic turtle brain. *Am J Physiol Regul Integr Comp Physiol* **275**, R2023–2027.

Pérez-Pinzón M, Rosenthal M, Sick T, Lutz P, Pablo J & Mash D (1992). Downregulation of sodium channels during anoxia: a putative survival strategy of turtle brain. *Am J Physiol Regul Integr Comp Physiol* **262**, R712–715.

Prentice HM, Milton SL, Scheurle D & Lutz PL (2003). Gene transcription of brain voltage-gated potassium channels is reversibly regulated by oxygen supply. *Am J Physiol Regul Integr Comp Physiol* **285**, R1317–1321.

Reuss ML, Rudolph AM & Heymann MA (1981). Selective distribution of microspheres injected into the umbilical veins and inferior vena cavae of fetal sheep. *Am J Obstet Gynecol* **141**, 427–432.

Robinson S, Petelenz K, Li Q, Cohen ML, DeChant A, Tabrizi N, Bucek M, Lust D & Miller RH (2005). Developmental changes induced by graded prenatal systemic hypoxic-ischemic insults in rats. *Neurobiol Dis* **18**, 568–581.

Rodríguez de Lores Arnaiz G (2000). How many endobains are there? *Neurochem Res* **25**, 1421–1430.

Rosenkrantz TS, Kubin J, Mishra OP, Smith D & Delivoria-Papadopoulos M (1996). Brain cell membrane Na^+,K^+-ATPase activity following severe hypoxic injury in the newborn piglet. *Brain Res* **730**, 52–57.

Rougier JS, Van Bemmelen MX, Bruce MC, Jespersen T, Gavillet B, Apotheloz F, Cordonier S, Staub O, Rotin D & Abriel H (2005). Molecular determinants of voltage-gated channel regulation by the Nedd4/Nedd4-like proteins. *Am J Physiol Cell Physiol* **288**, C692–701.

Sallmann FR, Bourassa S, Saint-Cyr J & Poirier GG (1997). Characterization of antibodies specific for the caspase cleavage site on poly (ADP-ribose) polymerase: specific detection of apoptotic fragments and mapping of the necrotic fragments of poly (ADP-ribose) polymerase. *Biochem Cell Biol* **75**, 451–456.

Teitel DF, Iwamoto HS & Rudolph AM (1987). Effects of birth-related events on central blood flow patterns. *Pediatr Res* **22**, 557–566.

Towbin H & Gordon J (1984). Immunoblotting and dot immunobinding-current status and outlook. *J Immunol Meth* **72**, 313–340.

Wei L, Yu SP, Gottron F, Snider BJ, Zipfel GJ & Choi DW (2003). Potassium channel blockers attenuate hypoxia- and ischemia-induced neuronal death *in vitro* and *in vivo*. *Stroke* **34**, 1281–1286.

Xia Y & Haddad GG (1999). Effect of prolonged O_2 deprivation on Na^+ channels: differential regulation in adult versus fetal rat brain. *Neuroscience* **94**, 1231–1243.

Zar JH (1984). *Biostatistical Analysis*, 2nd edn, pp. 185–205. Prentice Hall, Englewood Cliffs, NJ, USA.

Zauner A, Di Bullock RX & Young HF (1995). Brain oxygen, CO_2, pH, and temperature monitoring: evaluation in the feline brain. *Neurosurgery* **37**, 1168–1176.

Acknowledgements

We are very grateful to Dr María Serón Ferré, Dr Julian T. Parer and Dr Claudia Torres-Farfan for their invaluable help in preparing this manuscript, and to Carlos Brito and Mario Morales for their skilful technical assistance. FONDECYT N°1020599 and 7030057 funded this work in Chile.